

Interactions of Galaxies outside Clusters and Massive Groups

Jaswant K. Yadav^{1*}, Xuelei Chen^{1,2}

¹*National Astronomical Observatories, Chinese Academy of Sciences, 20A Datun Road, Chaoyang District, Beijing 100012, China*

²*Center of High Energy Physics, Peking University, Beijing 100871, China*

17 June 2014

ABSTRACT

We investigate the dependence of physical properties on small and large scale density environment. The galaxy population consists of mainly passively evolving galaxies in comparatively low density regions of Sloan Digital Sky Survey (SDSS). The environment is defined by (i) local density using adaptive smoothing kernel, (ii) projected distance, r_p , to the nearest neighbor and (iii) the morphology of the nearest neighbor. In order to detect long-range interaction effects we divide galaxy interactions into four cases depending on morphology of target and neighbor galaxies. We report that the impact of interaction on galaxy properties is detectable at least out to the pair separation corresponding to the virial radius of (the neighbor) galaxies in our sample, which is mostly between 210 and 360 h^{-1} kpc. We show that early type fraction, for isolated galaxies with $r_p > r_{vir,nei}$ are almost ignorant of the background density and, has a very weak density dependence for closed pairs. Star formation activity of a galaxy is found to be crucially dependent on neighbor galaxy morphology. We find star formation activity parameters and structure parameters of galaxies to be independent of the large scale background density. We also exhibit that changing the absolute magnitude of the neighbor galaxies does not affect significantly the star formation activity of those target galaxies whose morphology and luminosities are fixed.

Key words: galaxies: evolution galaxies: formation galaxies: fundamental parameters galaxies: general

1 INTRODUCTION

One of the key feature of the hierarchical picture of galaxy formation and growth involves continuous interactions and mergers with other galaxies. Various galaxy properties such as morphology, luminosity, structure parameters, star-formation rate (SFR) and dust properties are strongly affected by these interactions (Struck 2006; Woods & Geller 2007; Blanton & Moustakas 2009). The location of galaxies in particular environment is known to significantly affect their physical properties (Hubble 1936; Oemler 1974; Dressler 1980; Postman & Geller 1984; Kauffmann et al. 2004; Blanton et al. 2005b; Weinmann et al. 2006; Blanton & Berlind 2007; Lambas et al. 2012). With the advent of large spectroscopic and photometric surveys, the study of the role of the environment in galaxy formation has got a new impetus (Balogh et al. 2004; Park et al. 2007; Cooper et al. 2006; Cucciati et al. 2006; Skibba et al. 2012). With the availability of large galaxy samples, such as Sloan Digital Sky Survey Data Release 7 (SDSS-DR7 Abazajian et al. 2009), we are in a position to explore many dimensions of galaxy properties simultaneously and homogeneously. This kind of analysis helps us put galaxy scaling relationships in context with respect to one another as well as probe the underlying physics affecting galaxy formation and evolution.

Starting from the suggestions of Toomre (1977) that elliptical galaxies can be formed by the merger between spiral galaxies, there is growing evidence for a change in galaxy morphology (e.g. Park et al. 2008; Buta 2013) and galaxy structure as a result of merger (e.g. Nikolic et al. 2004; Patton et al. 2005; Hernández-Toledo et al. 2005; Park & Choi 2009). On the other hand, at fixed color, the residual dependence of galaxy morphology on environmental density is reported to be rather weak (Ball et al. 2008; Bamford et al. 2008). With an earlier release of SDSS data (DR4) Park et al. (2008) showed that when a galaxy is located within the virial radius of its nearest neighbor, its morphology tends to be the same as that of the neighbor. This points to an important role of hydrodynamic interactions with neighbors within the virial radius. Further studies comprising of galaxies in galaxy clusters (Park & Hwang 2009; Cervantes-Sodi et al. 2011), and involving hosts and their satellite galaxies (Ann et al. 2008; Wang et al. 2010) seem to favor this proposition.

In regard to star formation activity, following Zwicky's suggestion that collisions would be frequent within dense galaxy clusters, Spitzer & Baade (1951) argued that strong shock waves could push the interstellar gas out of these galaxies resulting in scarcity of late-type spiral galaxies with substantial ongoing star formation in clusters. Larson & Tinsley (1978) identified interacting galaxies from Atlas of Peculiar Galaxy, and determined that many of these galaxies had recently undergone a burst of star formation (see also

* E-mail: jaswant@nao.cas.cn

McQuinn et al. 2010). Several groups (e.g. Condon et al. 1982; Keel et al. 1985; Kennicutt et al. 1987) have observed and found bursts of star formation associated with tidal interactions. Barton et al. (2007) constructed an isolated “field” galaxy mock sample using cosmological N-Body simulations and compared it with “field” galaxy sample from 2dF data to establish that a large fraction of the galaxies that experience close passes respond with triggered star formation. Tonnesen & Cen (2012) find the tendency of close pairs in high-density environments to have fewer low specific SFR galaxies than non-pairs, whereas pairs in low-density environments have the opposite trend. Star formation related properties, such as color and emission-line flux, are found to be directly correlated with environmental density (Kauffmann et al. 2004; Blanton et al. 2005b; Christlein & Zabludoff 2005; Patton et al. 2011; Ideue et al. 2012). In addition, SFR and the fraction of star-forming galaxies is reported to be decreasing with increasing galaxy density (Carter et al. 2001; Lewis et al. 2002; Gómez et al. 2003; Mateus & Sodré 2004; Mahajan et al. 2010; Ellison et al. 2011).

Regarding studies of structure parameters of galaxies, Bretherton et al. (2013) studied the normalized rates and radial distributions of star formation in galaxies within low-redshift clusters to report that morphological type classifications of cluster galaxies correlate only weakly with their concentration indices, whereas this correlation is strong for non-cluster populations of disk galaxies. Park & Choi (2009) studied the variation of velocity dispersion and found almost no change for early type galaxies while for late type galaxies the velocity dispersion becomes larger as they approach their neighbors. Huertas-Company et al. (2013) report that at intermediate redshifts, the size-mass relation for passive early-type galaxies is independent of environments ranging from field to groups which seem to contradict the findings by Cooper et al. (2012) at similar redshifts. Lani et al. (2013) find that the massive quiescent galaxies at $z > 1$ are typically 50% larger in the highest density environments compared to those in the lowest density environments whereas this relationship between size and environment is much weaker for star-forming galaxies.

In addition to small scale dependence of galaxy properties discussed above, there are different studies which determine the dependence of various galaxy properties on large-scale structure (Binggeli 1982; White et al. 2010). Einasto et al. (2007) reported higher fraction of early type, passive, red galaxies in rich superclusters compared to poor superclusters thereby indicating the role of global environment in influencing galaxy morphology and their star formation activity (see also Patel et al. 2011; Lietzen et al. 2012). Park et al. (2007), however, concluded that different galaxy properties are independent of large-scale density once morphology and luminosity are fixed (see also Park & Choi 2009; Kajisawa et al. 2013).

The extent to which the galaxy properties are driven by internal-physical-processes (*‘nature’*) as opposed to external-physical-processes (*‘nurture’*) is still a matter of debate (Harrison et al. 2011). A sample of galaxies whose physical properties are largely the result of internal-physical-processes can be used to address this issue in greater details. By comparing the physical properties of these galaxies in different environments we can have a better idea of the role played by nurture-induced processes. Keeping this in mind, for this work, we use a subsample of galaxies from SDSS-DR7 which are neither in the vicinity of a member of Abell Cluster of galaxies nor a part of large group of galaxies. The three-dimensional environment parameter space, used in this study, enables us better understand the effects of galaxy interactions.

A brief outline of the paper follows. In section 2 we describe

the data from Sloan Digital Sky Survey. Different subsections describe associated morphology classification, small and large scale density environments as well as definition of nearest neighbor galaxy as used in our analysis. The results of environment dependence of different galaxy properties are presented in detail in section 3. We conclude this paper with discussions and conclusions in section 4.

2 DATA

2.1 SDSS Galaxy Sample

We use galaxies from the SDSS-DR7. This data release covers about 8,032 square degrees in the northern sky and consists of a series of three interlocking imaging and spectroscopic surveys. A 2.5m telescope located at Apache Point Observatory in Southern New Mexico is being used to carry out observations in five photometric bands ranging in wavelength from 3000 to 11000 Å (Fukugita et al. 1996; Gunn et al. 1998). After careful photometric image reduction, calibration and classification of individual galaxies, a subsample of galaxies with Petrosian r band magnitude $r < 17.77$ has been chosen for follow up spectroscopic observations (Lupton et al. 1999, 2001; Strauss et al. 2002). The spectroscopic sky survey is being performed using two multi-object fiber spectrographs on the same telescope. Each spectroscopic fiber plug plate having a circular field-of-view, with a radius of 1.49 degrees, can accommodate a total of 640 fibers. Because of the finite size of the fiber plugs, the minimum separation of fiber centers is $55''$. If two galaxies are within $55''$ of each other, both of them can be observed only if they lie in the overlap between two adjacent fiber plug plates (Blanton et al. 2003).

For the present study we use the Korea Institute for Advanced Study Value-Added Galaxy Catalog (KIAS-VAGC) (Choi et al. 2010). This catalog has been extracted from the New York University Value-Added Galaxy Catalog (NYU-VAGC) Large Scale Structure Sample (brvoid0) (Blanton et al. 2005) that includes 583,946 galaxies within a r band apparent magnitude range of $10 < r < 17.6$. Our sample is supplemented by brighter galaxies that are not part of SDSS and whose redshifts are obtained from various literatures (Choi et al. 2007). This leads to a total of 707,817 galaxies in the flux limited sample. Such a large catalog of galaxies offers the advantage of an extended magnitude range with high completeness.

The volume limited sample used for the present study is a galaxy sample with r -band absolute magnitude $M_r < -19.0 + 5 \log h$ and redshifts $0.020 < z < 0.074$ or a comoving distance of $59.7 h^{-1} \text{Mpc} < d < 218.9 h^{-1} \text{Mpc}$. This sample includes 114272 galaxies. In order to select, mainly passive galaxies from low density environments, we post process the volume limited sample by removing galaxies within a velocity separation of $\pm 3000 \text{ km s}^{-1}$ and a projected separation of 3 Mpc from galaxies located inside Abell Clusters (Abell et al. 1989) of galaxies. Furthermore we apply finger of god corrections (Bahcall et al. 1986) to galaxies belonging to SDSS group catalog of Yang et al. (2007) and remove galaxies which are member of massive groups. This is done to minimize the effects of large scale density environments on various galaxy properties. In principle, the property of a galaxy may be affected by more than one neighbor galaxy. For the present study a target galaxy that is within virial radius of its second nearest neighbor (refer to 2.4) is also removed from sample. The removal enables us to better understand the effect of “the nearest neighbor” on differ-

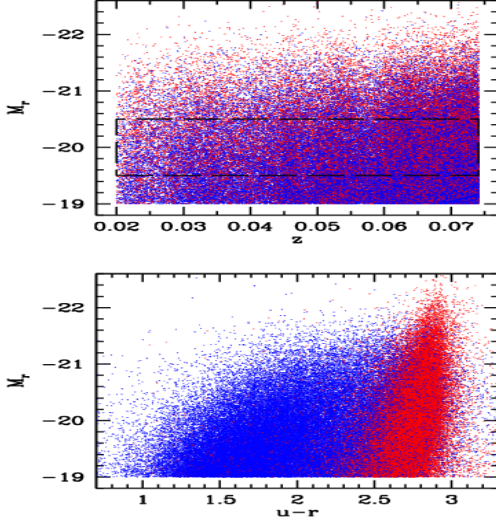


Figure 1. The rectangular box in the upper panel encloses the target galaxies which are part of a total of 114,272 galaxies contained in our volume limited subsample. The faint limit of these target galaxies is 0.5 mag brighter than the full sample to achieve complete neighbor selection. The bottom panel shows the galaxies in the *color – magnitude* diagram. Red points are early–morphological–type galaxies and blue points are late types.

ent galaxy properties. The subsample of galaxies is plotted in figure 1.

2.2 Morphology Classification

Park & Choi (2009) stressed the importance of accurate morphology classification since the effects of interaction strongly depend on morphology of interacting galaxies. For this work we use Park & Choi (2005) prescription to classify morphological types of galaxies in our sample. In this scheme the the location of galaxies, in the color-color gradient space, combined with their i-band concentration enables us in dividing the sample into early (ellipticals and lenticulars) and late (spirals and irregulars) morphological types with completeness and reliability of sample around 90%. An additional visual check of color images is undertaken to account for possible incorrect morphological classification of about 10,000 galaxies having close neighbors. This is necessary because Park & Choi (2005) prescription performs poorly when an early-type galaxy starts to overlap with other galaxies. Visual analysis guides us in identifying blue but elliptical-shaped, and dusty edge-on spiral galaxies. It is also useful in correcting central positions of merging galaxies. These procedures result in a volume limited subsample of 114,272 galaxies with $M_r < -19.0$. Removing the galaxies that are, part of massive SDSS groups (Yang et al. 2007), in the vicinity of Abell Clusters or are near the survey boundaries result in a population of 86,604 galaxies out of which 30,298 are early-type, and the rest are late-type galaxies.

Different properties of galaxy population are studied in the absolute magnitude range of $-19.5 > M_r > -20.5$. In such a subsample volume we have 14,244 early types and 25,771 late types. We identify these galaxies as those lying within a rectangular box in Figure 1. As argued in literature (see e.g. Choi et al. (2007); Park & Choi (2009)), in order to minimize the effect of internal extinction on different galaxy properties, we restrict our late-type galaxy

population to those having an isophotal axis ratio greater than 0.6. This results in a further reduction of late-type galaxies to 14,581 within the absolute magnitude limit of our subsample. Different physical properties of galaxies are studied by subdividing the sample of galaxies into four subsamples: 7106 early types having early type nearest neighbor (the E–e galaxies), 7138 early types having late-type nearest neighbor (E–l), 6894 late types having early-type nearest neighbor (L–e), and 7687 late types having late-type nearest neighbor (L–l).

2.3 Environment

There is a variety of methods to measure galaxy environment that may or may not correlate with each other (Muldrew et al. 2012). We have followed Park & Choi (2009) in defining three different environment measures namely large-scale background density, small-scale mass density and morphology of the closest neighbor galaxy. In this scheme large scale background density at given location of an object in our sample is given by

$$\rho_{20}(\mathbf{x})/\bar{\rho} = \sum_{j=1}^{20} \gamma_j L_j W_j(|\mathbf{x}_j - \mathbf{x}|)/\bar{\rho} \quad (1)$$

where γ and L are mass to light ratio and luminosity of closest 20 galaxies around an object in our volume limited sample. The weighting, W , is defined in terms of a spline kernel (Monaghan & Lattanzio 1985; Park et al. 2007) because it is adaptive, centrally weighted and has a finite tail, making it superior to tophat, cylindrical and Gaussian kernels. The smoothing scale determined by 20 nearest neighbor in our volume limited sample is larger than typical cluster virial radius (about $1.2h^{-1}\text{Mpc}$) resulting into an estimation of ρ_{20} that never exceeds the virialization density.

The small scale density experienced by a target galaxy due to local mass density given by its nearest neighbor is defined as

$$\rho_n/\bar{\rho} = 3\gamma_n L_n / 4\pi r_p^3 \bar{\rho} \quad (2)$$

with r_p being the projected separation of the nearest neighbor from target galaxy. In order to understand the interactions among various galaxies, we have studied the dependence of various galaxy properties on the projected separation from its nearest neighbor normalized by neighbor’s virial radius (see Figure 3,5,7). Following Park et al. (2008), we have defined the virial radius of a galaxy as the projected radius where the mean mass density within the sphere of radius r_p is 200 times the critical density of the universe. According to our estimates, the virial radii of galaxies with $M_r = -19.5, -20.0$ and -20.5 are $264.74, 308.66$ and $359.87h^{-1}\text{kpc}$ for early types and $210.12, 244.98$ and $285.63h^{-1}\text{kpc}$ for late types, respectively. Clearly, the virial radius thus defined includes the galaxy as well as the surrounding dark matter halo region.

2.4 The Nearest Neighbor

The definition of nearest neighbor galaxy in our study is similar to the one in Park & Choi (2009). It requires the neighbor to be situated closest to the galaxy on the sky satisfying absolute magnitude and radial velocity conditions as well. The absolute magnitude condition requires the difference between neighbor and target galaxy’s absolute magnitude to be smaller than ΔM_r and larger than $\Delta M_r - 1$. For most of the work we chose ΔM_r to be 0.5. We also discuss, in section 4, the dependence of galaxy properties on a range of values of ΔM_r . The radial velocity condition demands that the neighbor galaxy must lie within $\pm 600(800)\text{kms}^{-1}$ if the

target is late(early) type. The velocity difference between target and neighbor galaxy should also depend on their luminosity (Faber & Jackson 1976; Tully & Fisher 1977) and projected separation. Accordingly velocity dispersion between early and late-type galaxies in our sample turns out to be between 1.3 to 1.4 across different separations (see Figure 2 of Park & Choi (2009) for details).

3 RESULTS

We study the variation of galaxy properties on distance to the nearest neighbor, morphology of the nearest neighbor and background density contributed by 20 neighbor galaxies. We leave out galaxies from very high density environments like Abell clusters and massive SDSS groups. For the galaxies in our subsample, we study different properties such as morphology, absolute magnitude, star formation activity (u-r color, g-i color gradient, equivalent width of the H α line) and structure parameters (central velocity dispersion, i-band Petrosian radius, concentration index).

For most portions of our study, we fix the r-band absolute magnitude of target galaxies in a narrow range between -19.5 and -20.5 . This enables restricting effects due to the coupling of a parameter with luminosity. As pointed out in Choi et al. (2007), late-type target galaxies with the i-band isophotal axis ratio less than 0.6 suffer from internal extinction and corresponding dispersion in luminosity. To avoid false trends in galaxy properties due to this issue, we have discarded such galaxies from our analysis.

Smooth distributions of various physical parameters in figure 4, 6 and 8 are found by the following method. At each point of parameter space, we first sort the values of physical parameter of galaxies contained within a certain spline radius from the point. The median value of a physical parameter is then given by the galaxy whose cumulative sum of spline kernel weights is $\sum w_i/2$, where w_i is the individual spline weight of a galaxy around that point. The median is preferred over mean because of possible skewness in the distribution of various physical parameters.

3.1 Morphology

We build our study on previous similar analysis (e.g. Park & Choi 2009; Park & Hwang 2009) of morphology dependence on local environment. With a much larger SDSS DR7 data sets we are in a position to study this dependence in greater details for galaxies lying in comparatively low density regimes. Figure 2 shows the variation of fraction f_E of early type galaxies as function of large scale background density (ρ_{20}) and projected separation r_p from the galaxy's nearest neighbor. Early (red dot) and late (blue dot) type galaxies, having early type (upper panel) and late type (lower panel) nearest neighbor, are distributed in a triangular shaped region in this figure. This is due to the statistical correlation between r_p and ρ_{20} . At each point of parameter space we obtain the value of f_E from the ratio of weighted number of early type galaxies to the weighted number of total galaxies within a smoothing spline kernel of fixed size. The contours thus obtained are restricted to regions with statistical significance above 1σ .

In case of target galaxies having early type neighbors (upper panel), we detect a gradual increase in f_E as the galaxy approaches its neighbor. For galaxies in our sample we find no (or very little) dependence of f_E on background density for galaxies that are situated outside (or inside) the virial radius of their neighbors, thus indicating the absence of any morphology density relation (Dressler

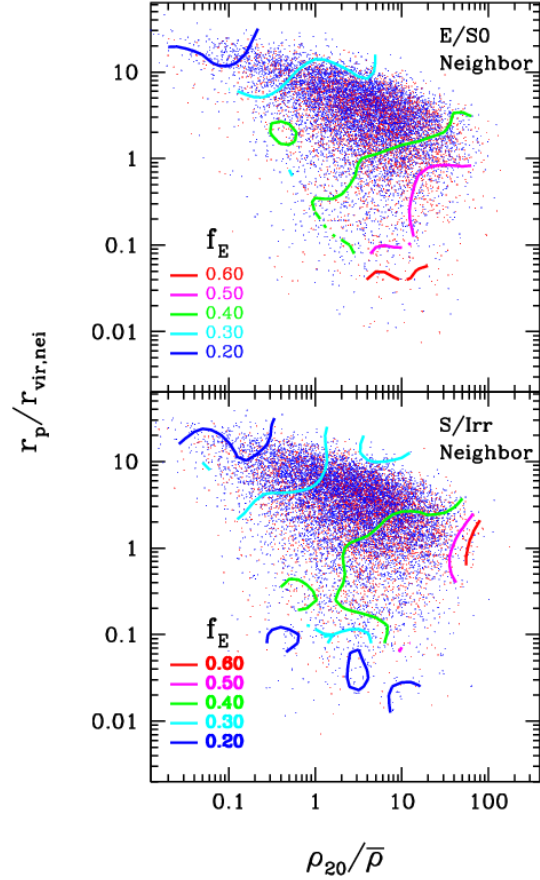


Figure 2. (Upper) Environment dependence of Morphology, when the nearest neighbor is an early-type galaxy. Red points are early-type target galaxies and blue points are late-type target galaxies. Absolute magnitude of galaxies is fixed to a narrow range of $-19.5 > M_r > -20.0$. Contours show constant early-type galaxy fraction f_E . Contours are limited to regions with statistical significance above 1σ . (Lower) Same, but for the late-type nearest neighbor case.

1980). The behavior of f_E for galaxies with late type nearest neighbor (lower panel) is similar at separations larger than neighbor's virial radius. However, when the galaxy is inside the virial radius of its neighbor, f_E starts decreasing after attaining a maximum value around $r_p \sim 0.3 r_{vir,nei}$. Significant hydrodynamic effects from neighbor galaxies appear to be important at these separations. Sensitivity of f_E to ρ_{20} exists mainly within the virialized region at very high background density. This verifies earlier studies (e.g. Park et al. 2008) confirming that the effects of the nearest neighbors are critically important to galaxy morphology.

In the region of low merger and interaction ($r_p > r_{vir,nei}$), we report an early type fraction that asymptotically approaches about 0.2. This could be the inborn morphology fraction. In such an environment, early type galaxies couldn't have formed by processes such as strangulation because of lack of nearby large galaxies. According to recent observational (Croton & Farrar 2008) and theoretical (Hirschmann et al. 2013) studies, such early type galaxies could either have formed due to AGN heating or other internal processes of galaxy formation.

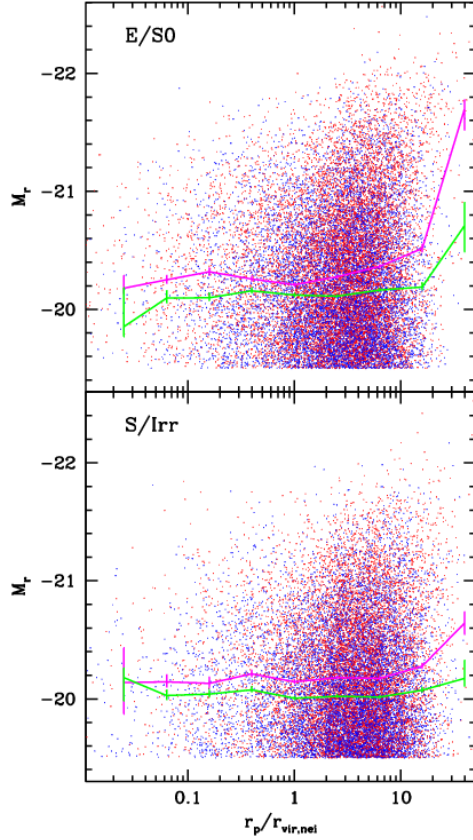


Figure 3. Absolute magnitude - Neighbor separation relation. The upper panel is for the early-type target galaxies, and the lower panel is for late types. All galaxies brighter than $M_r = -19.5$ are plotted. The median M_r relations are drawn for early-type neighbor (red dots, magenta line) and late-type neighbor (blue dots, green line) cases.

3.2 Luminosity

Figure 3 shows the r-band absolute magnitudes of all galaxies in a volume-limited sample with $z < 0.0741$ and $M_r < -19.0$. The lines with error bars are the median values as a function of projected separation from nearest neighbor. We find that the absolute magnitude of galaxies with early type neighbors is much brighter than those with late type neighbors. The neighbor separation does not seem to affect this behavior except for L-I, in which case the magnitude seem to rise as the galaxies come closer to each other.

Figure 4 examines the environmental dependence of M_r in the $r_p - \rho_{20}$ plane. We find that on smaller separation from the neighbor, i.e. at $r_p/r_{vir,nei} < 1$, the galaxies irrespective of their morphology show no variation in M_r as a function of separation and almost none to very little (~ 0.2) variation with respect to the underlying density field. At much smaller separation, we also observe a tendency for a galaxy to have neighbor of same morphology, which is indicated from a lesser population of $E-l$ galaxies compared to $E-e$ galaxies. Park et al. (2008) & Park & Choi (2009) have earlier reported an early to late type morphology transformation which we can explain by larger number of $L-l$ galaxies in comparison to $E-l$ galaxies at the scale of hydrodynamic interactions. Such a transformation can be explained by transfer of cold gas from late type neighbors to their early type target galax-

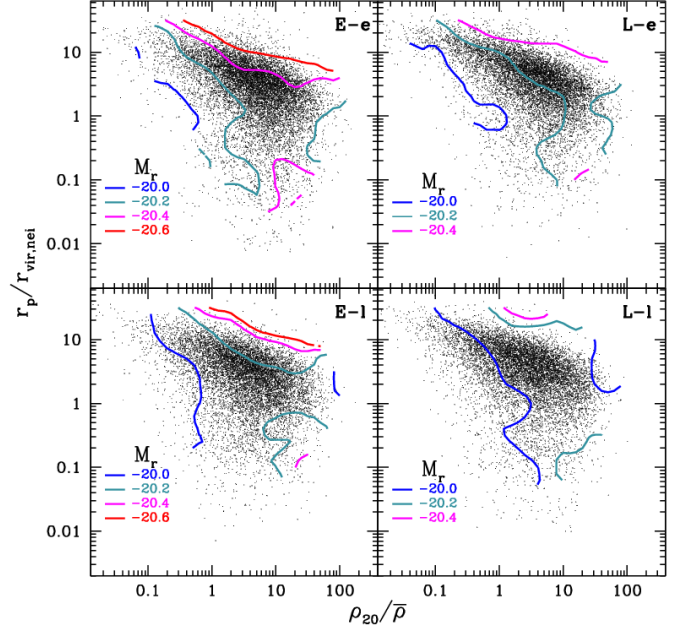


Figure 4. Three dimensional (morphology, r_p and ρ_{20}) environment dependence of Median absolute magnitude. Points are all target galaxies brighter than $M_r = -19.5$. Four cases are given, the early-type target galaxies having an early-type neighbor (E-e), early-type targets having a late-type neighbor (E-l), late-type targets having an early-type neighbor (L-e), late-type targets having a late-type neighbor (L-l).

ies through interactions, thereby changing the morphology of early type galaxies to late type.

However when the galaxies are well separated from their neighbor, we find significant dependence on both separation as well as density field. In such a situation, we find that galaxies that are farther from their neighbors tend to be the brighter one. The luminosity decreases as the galaxies come closer at this separation and this behavior is more apparent in high density environments. In the low density environments the variation with respect to $r_p/r_{vir,nei}$ is slow possibly because of fewer number of neighbors (Park & Choi 2009). Another observation from figure 4 helps us to infer that higher luminosity contours have negative slopes, indicating that the change in M_r due to ρ_{20} is much faster when the galaxies are at comparatively larger separation.

3.3 Star Formation Activity Parameters

The $u-r$ color of a galaxy is a measure of the star formation activity of galaxies in the recent past. Equivalent width of $H\alpha$ line is a well calibrated standard indicator of star formation rate (Kennicutt 1998). This width can be defined as the ratio of the $H\alpha$ luminosity to the underlying stellar continuum thus representing a measure of the the current to past average star formation. It is therefore a model independent, directly observed proxy for specific star formation rate of a galaxy. The color gradient of a galaxy enables us to study the star formation history along the disk. The u -band surface photometry of galaxies in our sample is noisy. For this reason we use gradient in $g-i$ color which has been corrected for the inclination and seeing effects. It is defined as the difference in $g-i$ color between the central and annulus region of the galaxy

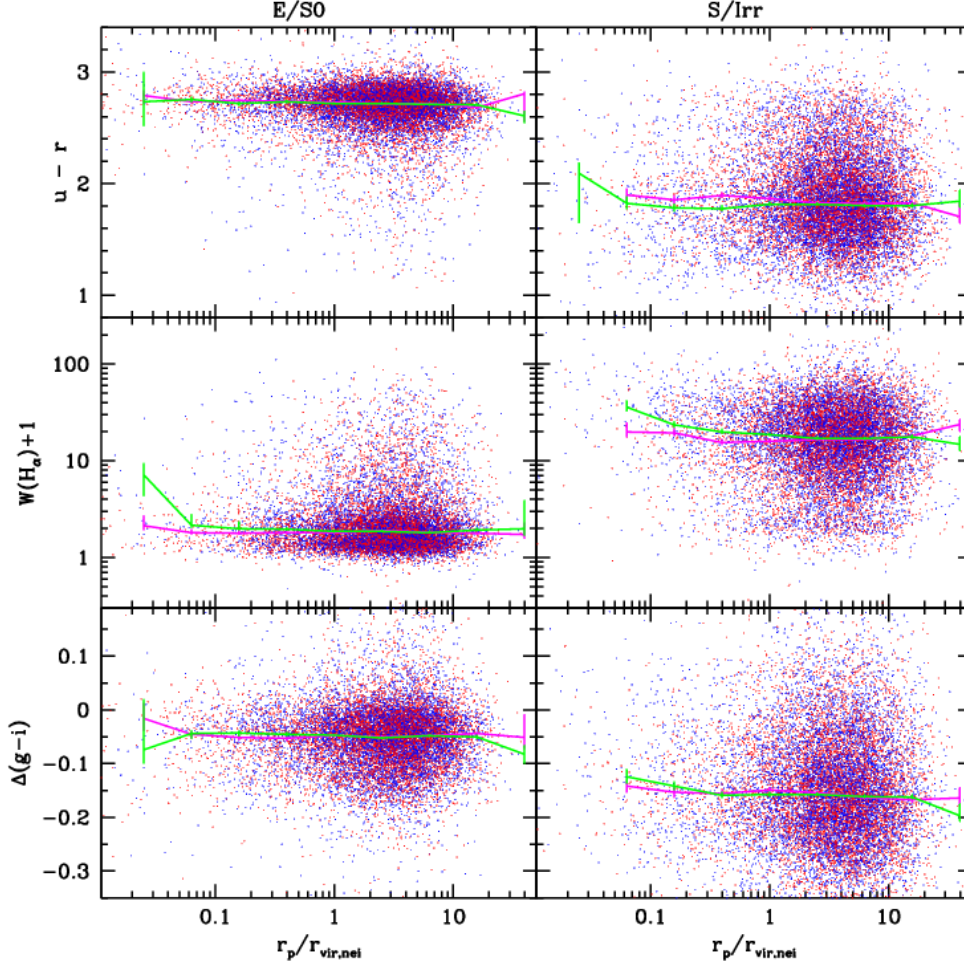


Figure 5. Star formation activity parameters of our target galaxies with $-19.5 > M_r > -20.5$ and their dependence on the distance to the nearest neighbor normalized to the virial radius of the neighbor. Left panels are for early-type target galaxies and right panels are for late types. Median curves are drawn for the cases of early-type neighbor (magenta line, red dots) and of late-type neighbor (green line, blue dots). The r_p -space is uniformly binned in the logarithmic scale, and in each bin, the median value of physical parameter of the galaxies belonging to the bin is used for the median curve.

in our sample. Observational studies indicate that the higher surface brightness galaxies have shallower color gradients. Figure 5 shows the distribution of $u-r$ color, equivalent width of $H\alpha$ line and $g-i$ color gradient of galaxies divided according to their neighbor morphology as a function of $r_p/r_{vir,nei}$. The left(right) panels are for early(late) type target galaxies. Dots in Figure 5 and 6 are the galaxies with $-19.5 \geq M_r > -20.5$ spread in the two and three dimensional environmental parameter space respectively.

Figure 5 shows the radial dependence of the star formation activity parameters. We find that when the target galaxy is early type its median $u-r$ color is constant, irrespective of the neighbor's morphology or separation. For late type target galaxies the $u-r$ color is slightly larger for those with early type neighbors. On smaller separations the late type galaxies having late type neighbors show an increase in their $u-r$ color, however, the sample size becomes so small that the increase is not statistically significant. In line with the constancy of $u-r$ color, the equivalent width of $H\alpha$ line for early type galaxies is constant and indistinguishable of neighbor's morphology at separations larger than $0.1 r_{vir,nei}$ as shown in mid-

dle row of figure 5. The situation is completely different when the neighbor morphology is late type. When any galaxy comes within the virial radius of its late type neighbor it shows a dramatic increase in its SFA. Park & Choi (2009) had noticed a sharp drop in SFA of a late type galaxy when it came in close contact with early type galaxy. We, however, don't see such a dramatic drop possibly because our galaxies are mainly taken from low density regions compared to the sample used in Park & Choi (2009). The increase in width of $H\alpha$ line can be attributed to the interactions, however small, that are going on in these galaxies even though they reside in comparatively low density environments. The gradient in $g-i$ color, as shown in the lowest panel, slightly increases as the galaxy approaches its neighbor. This indicates that central region of galaxies become slightly bluer compared to the outside region. Different neighbor morphology do not seem to affect this behavior significantly unlike the case of $W(H\alpha)$ and $u-r$ color.

In order to better understand the dependence of these physical parameters on different environment parameters, in Figure 6, we study their behavior in three dimensional space indicated by large

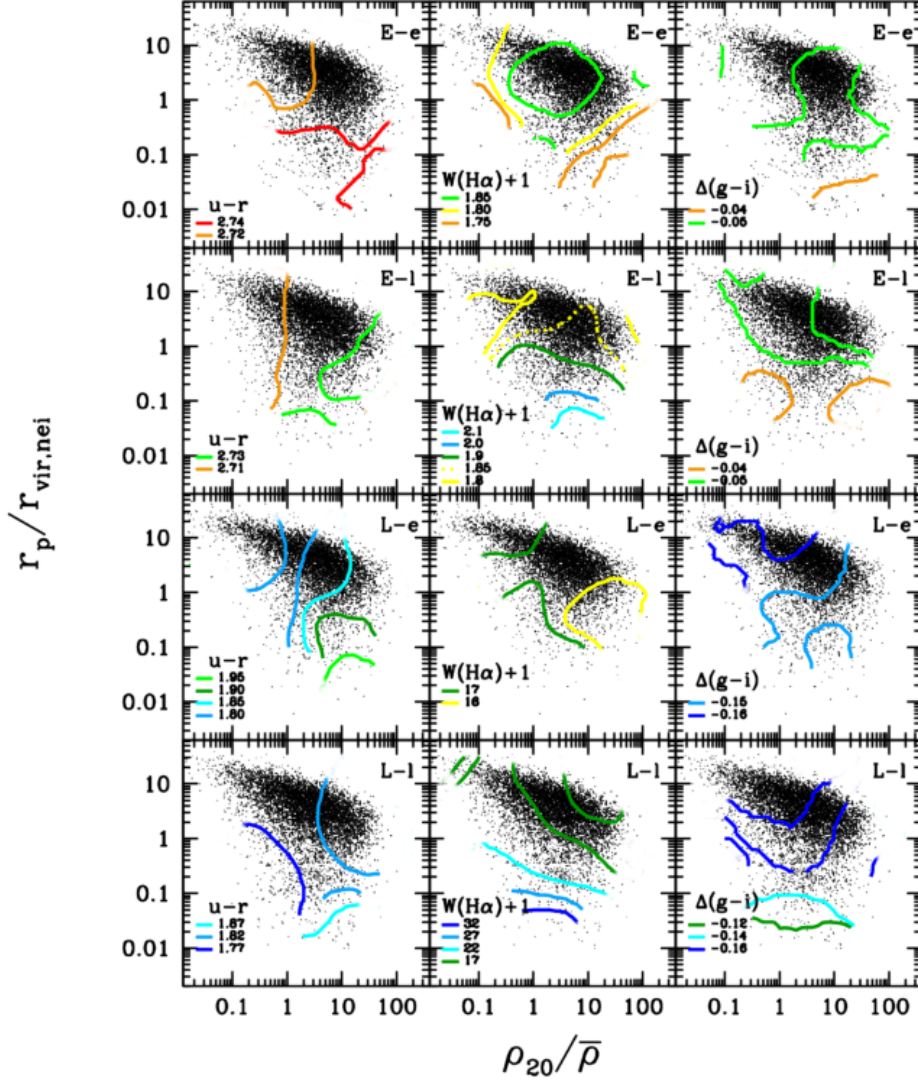


Figure 6. Variation of $u - r$ color, equivalent width of the $H\alpha$ line, $g - i$ color gradient of galaxies with $-19.5 > Mr > -20.5$ with respect to the pair separation r_p and the large-scale background density ρ_{20} . In each column, target galaxies are divided into four cases: the E-e, E-l, L-e, and L-l galaxies, respectively. Dots are galaxies belonging to each subset. At each location of the $r_p - \rho_{20}$ space, the median value of the physical parameter is found from those of galaxies within a certain distance from the location. Curves are the constant-parameter contours

scale background density, projected separation from the neighbor and neighbor's morphology. The $u - r$ color for early type target galaxies changes little as we traverse the full $\rho_{20} - r_p$ parameter space in the top left panels of Figure 6. For early type neighbor (E - e) and late type neighbors (E - l) the color changes by 0.02 remaining constant when the target galaxy is outside virial radius of its nearest neighbor. As the galaxy enters the virial radius of the neighbor, the color decreases slightly and shows a weak dependence on ρ_{20} for E - l case. The decrease in color on small scales for E - l galaxies is consistent with our findings of decrease in early type fraction on smaller scales in lower panel of figure 2. For late type target galaxies with early type neighbors, the $u - r$ color increases as the galaxies come closer to each other within the virial radius. Outside the virial radius the color does not change with r_p but shows a weak dependence on ρ_{20} . For the case of L-l, we notice

a peculiar increase in color as the galaxies come closer in the comparatively denser regions. In lower density regions, however, the color remains constant as a function of separation between nearest neighbors. We can conclude that color of early type galaxies remain constant as a function of small and large scale environment but for late type galaxies, we observe a weak but non zero dependence on underlying density field. Three dimensional contours of $W(H\alpha)$ show an even clearer dependence of neighbor separation and morphology. The middle column in figure 6 shows that SFA of early type galaxies with early type neighbors in intermediate density field does not depend on either density or the neighbor separation. In the comparatively lower as well as higher density regions there is a slight decrease in star formation activity as the galaxies come closer. The situation is similar for L - e case where we notice a slight decrease in $W(H\alpha)$ in high density regions. For the

E - l case, we notice a complete independence from local density in all density environments. At separations larger than virial radius, $W(H\alpha)$ remains constant but as the galaxy enters the virial radius of the late type neighbor $W(H\alpha)$ shows a gradual increase. This situation is similar to L - l case, except the increase in equivalent width $W(H\alpha)$ is almost double at close separation to what it was at separations beyond the virial radius. In the right column of Figure 6 contours represent the distribution of the median $\Delta(g - i)$ at each location of the r_p - ρ_{20} space. The color gradient $\Delta(g - i)$ of all galaxies irrespective of neighbor morphology is independent of density as can be seen from the horizontal contours. In case of E - e, E - l and L - e galaxies we notice a change in $\Delta(g - i)$ of about 0.01 for well separated and closeby neighbor galaxies. When a late-type galaxy approaches another late type neighbor inside its virial radius, its color gradient increases (center becomes relatively bluer) significantly compared to three other cases. (see Figs. 6 and 7 of Park & Choi 2009).

3.4 Structure Parameters

Concentration indices provide a quantitative determination of the radial distribution of light in specified passbands that is both useful in itself, and also provides a more objective indicator of galaxy type than is provided by, for example, Hubble classifications (Shimasaku et al. 2001; Strateva et al. 2001). Central velocity dispersion refers to the velocity dispersion of the interior regions of an extended object like galaxy or cluster of galaxies. Taking into account finite resolution of the SDSS spectrograph, the most probable velocity dispersion is restricted to galaxies with $\sigma > 40 \text{ km s}^{-1}$ (Choi et al. 2007). Physical parameter representing size of the galaxy is the Petrosian radius obtained from i -band images of galaxies.

Top row in figure 7 shows that radial dependence of concentration on morphology of the target galaxy. For early type target galaxies (left panel) the concentration is almost constant as a function of separation from neighbor whereas for late type targets (right panel) it increases (c_{in} decreases) as the target galaxy approaches the neighbor within its virial radius. This may be due to smaller size and compactness of the early type galaxy resulting in them being tidally more stable. The larger size and lower concentration of late type galaxies compared to their early type counterparts makes the former tidally more vulnerable, resulting in a higher concentration of late type galaxies as they approach their neighbors within the virial radius. The significant drop in inverse concentration ratio in case of late type galaxies with late type neighbors can also result from relatively smaller velocity difference between the target and neighbor galaxy, resulting in larger tidal energy deposits. Variation in central velocity dispersion as a function of neighbor separation follows similar pattern as concentration of galaxies. As indicated by middle row in figure 7, σ is almost independent of neighbor separation for early type galaxies (left panel) and increases as the late type galaxies approach their neighbor well within their virial radius (right panel). This behavior can once again be explained by compact, fast and tidally more stable nature of early type galaxies. The large deposits of tidal energy in case of late-late galaxy pairs can give rise to an increase in velocity dispersion as the pairs come closer (Binney & Tremaine 1987). The size dependence of a galaxy in terms of neighbor separation is shown in the bottom row of figure 7. The inclination and seeing corrected size of galaxies located in low density regions of the Universe does not show any variation as a function of neighbor separation for different combinations of target and neighbor morphology.

A three dimensional dependence of various structural param-

eters on morphology, large scale background density ρ_{20} and projected separation from the neighbor r_p is shown in figure 8. The left column shows the variation of i -band inverse concentration ratio of galaxies. As expected we observe a very weak decrease of inverse concentration as the target elliptical galaxy approaches its neighbor galaxy attaining a weak maximum for E - e case. For late type target galaxies, however, the decrease of c_{in} is comparatively stronger for decreasing r_p . For different combinations of target and neighbor galaxies, we find c_{in} to be independent of ρ_{20} . The decrease in c_{in} of late type galaxies at smaller neighbor separation has also been reported in Park & Hwang (2009) who analyzed a sample of galaxies in relatively denser environment. Effect of various environments on central velocity dispersion σ is shown in middle column of Figure 8. We observe a weak dependence of σ on ρ_{20} when $\rho_{20} < \bar{\rho}$. For early type galaxies, σ slightly increases with ρ_{20} in the low and intermediate density regions at $r_p > r_{vir,nei}$. This behavior is consistent with similar findings using galaxies from earlier SDSS data release (Park et al. 2007; Park & Choi 2009). However, in the high density regions we do not find any dependence of σ on ρ_{20} . The E - e panel shows an increase in σ as galaxies come closer to each other at fixed ρ_{20} while in case of E - l we don't find any dependence of σ on r_p . For late type target galaxies we report a σ that is independent of r_p and ρ_{20} at separations larger than $\sim 0.1 r_{vir,nei}$. At closer separations σ increases as the separation decreases particularly for L - l galaxies. The right column of Figure 8 shows the dependence of galaxies size on neighbor separation and background density. For E - e panel we notice that the size of the galaxy slightly increases as it moves in a higher density region at separation larger than the virial radius of its neighbor. Inside the virial radius we report a fixed size for E - e galaxies. Park & Choi (2009) have reported a rapid increase in size of E - e galaxies at separations below $0.01 r_{vir,nei}$ but in our dataset such a merging sample of early type galaxies is absent. For the remaining cases also the size of galaxies does not show a significant change as the galaxy traverses the full r_p - ρ_{20} parameter space. Choi et al. (2007) reported a strong dependence of galaxy size on morphology and luminosity of the galaxy population. In this work we have fixed the morphology, restricted the change in magnitude to 1 mag and omitted galaxies from high density regions of the universe resulting into the measurements of petrosian radius that is essentially fixed across a range of background density and neighbor separation.

4 DISCUSSION AND CONCLUSIONS

In this paper we have studied various physical properties of mainly passively evolving field galaxies from low density regions of SDSS. Effects of the nearest neighbor distance, the nearest neighbors morphology, and the large-scale background density are examined. In order to better understand the effect of the nearest neighbor galaxy, we have removed all those galaxies from our analysis that lie within the virial radius of their second nearest neighbor. We have hoped to remove the biases in galaxy properties due to morphology misclassification by using an accurate automated morphology classifier (Park & Choi 2005) combined with careful visual inspection. Mass transfer between interacting galaxies (Toomre 1977) can help us better understand the reason for decrease in early type fraction of galaxies as the target galaxies approach a late type neighbor galaxy (see Figure 2) within their virial radius. In such a scenario, the early type galaxy can acquire cold gas from the late type neighbor enabling the former to form a disk and transform itself to a late type galaxy (Park et al. 2008). Figure 5 indicates that at fixed back-

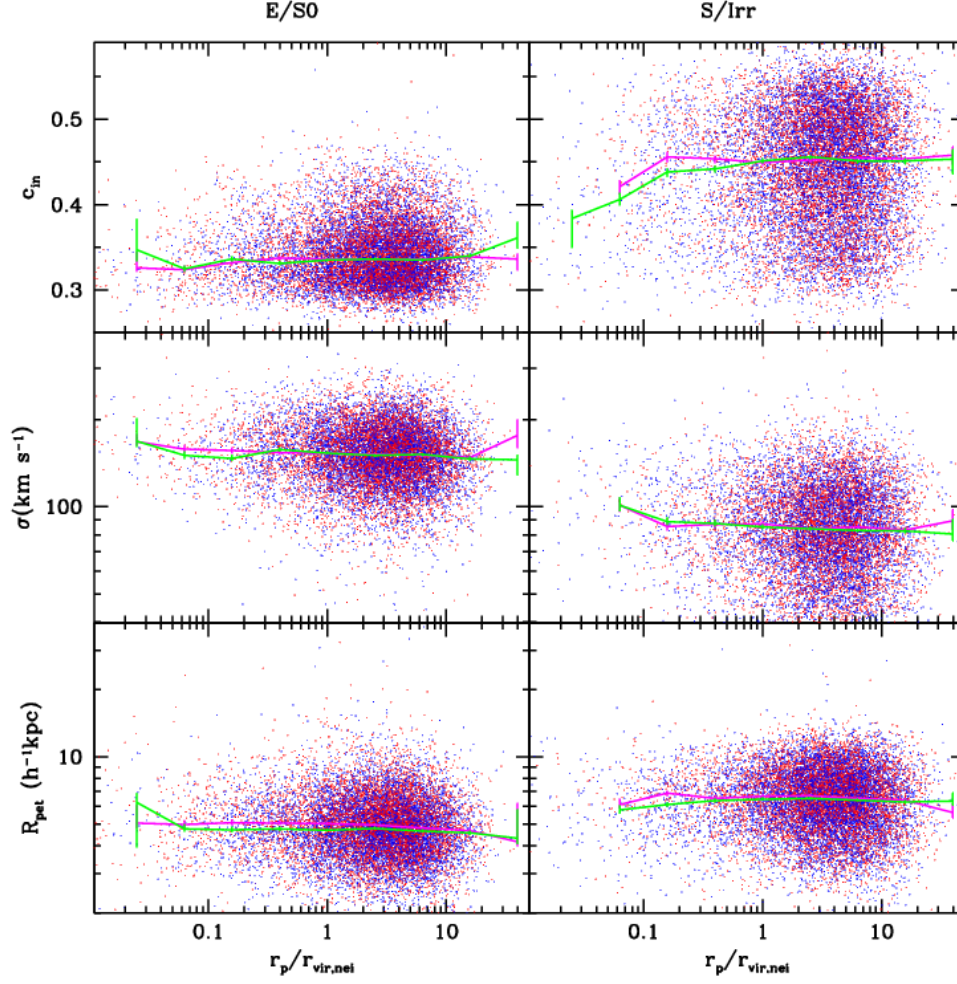


Figure 7. Structural parameters of our target galaxies with $-19.5 > M_r > -20.5$ and their dependence on the separation between the target galaxies and their nearest neighbor galaxy. The physical parameters considered here are the inverse concentration index c_{in} , central velocity dispersion σ , and Petrosian radius R_{Pet} . Left panels are for early types and right panels for late types. Cases are further divided into early-type neighbor (magenta median curves, red dots) and late-type neighbor (green curves, blue dots) cases.

ground density the isolated galaxies are comparatively brighter and among isolated galaxies the brighter ones lie in higher density environments. It can serve as the evidence of transformation of the galaxy luminosity class through the merger process. Our analysis reconfirms the importance of radius of the galaxy plus dark halo systems as a distance scale inside which most of the galaxy properties start to be sensitive to both the nearest neighbors distance and its morphology. The gravitationally bound pair of galaxies orbit each other within the virial radius resulting in repeated hydrodynamic interactions contributing to change in properties of the orbiting galaxies. Our study emphasize the importance of neighbor galaxy's morphology in either enhancing or suppressing of star formation activity (see e.g. middle column of Figure 6) of target galaxy which has long been assumed to only increase due to the internal mass perturbed by the tidal force of the neighbor (Kennicutt et al. 1987; Nikolic et al. 2004; Patton et al. 2011). Such a relation between morphology and star formation activity can be attributed to hydrodynamic interactions between approaching galaxies. Ram pressure effects experienced due to the collision with the

hot gas of the neighbor elliptical galaxy can explain the change in star formation activity of the late type galaxy. In order to analyze the robustness of our findings against the choice of neighbor selection parameter (ΔM_r), we restudied the behavior of equivalent width of $H\alpha$ line using different samples of galaxies that are constrained to have brighter as well as fainter neighbors than themselves. Figure 9 represents a scenarios in which the two distinct target galaxy populations exhibit similar behavior of $W(H\alpha)$ as a function of neighbor separation. Well inside the virial radius, $W(H\alpha)$ decreases slightly as we traverse the galaxy populations having fainter neighbors (solid cyan line, Figure 9) to those having brighter neighbors (dotted magenta line). We can fit the $W(H\alpha)$ as a function of $r_p/r_{vir,nei}$ using the function

$$W(H\alpha) = (31.37 \pm 5.50) \exp((-0.70 \pm 0.46) \frac{r_p}{r_{vir,nei}}) + C \quad (3)$$

where C is the measure of the value outside the virial radius of the neighbor. The slight decrease in $W(H\alpha)$ as a function of neighbor

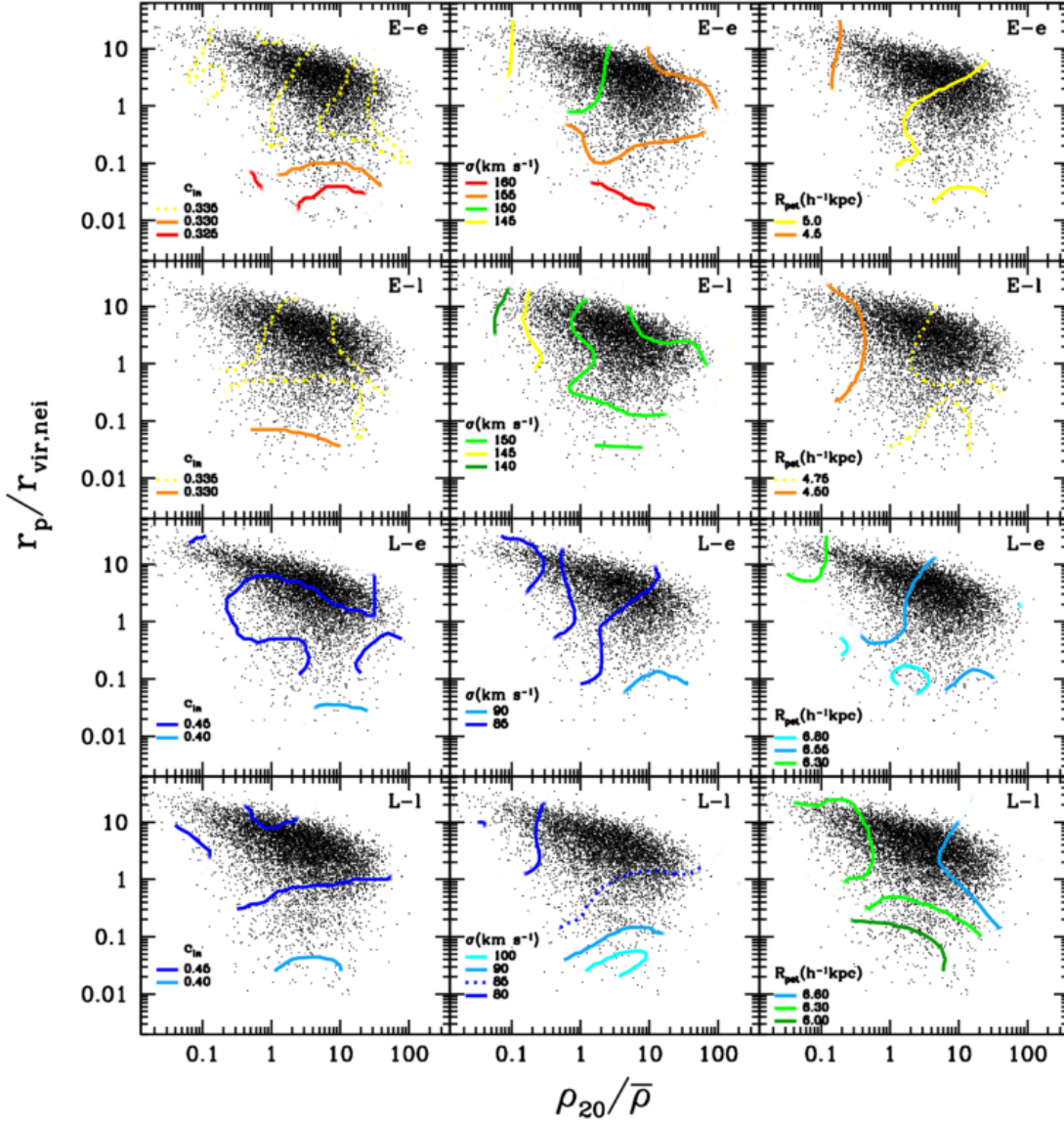


Figure 8. Three dimensional (morphology, r_p and ρ_{20}) environment dependence of the inverse concentration index c_{in} , central velocity dispersion σ and Petrosian radius R_{pet} of galaxies with $-19.5 > Mr > -20.5$. In each column, galaxies are divided into four cases: the E-e, E-l, L-e, and L-l galaxies, respectively. Dots are galaxies belonging to each subset. At each location of the $r_p - \rho_{20}$ space, the median value of the physical parameter is found from those of galaxies within a certain distance from the location. Curves are the constant-parameter contours

brightness for passive galaxies may be related to exchange of gas between interacting galaxies.

The additional role played by gravitational effects in the evolution of galaxies is evident by morphology independent structural parameter changes in Figure 7 as a function of neighbor separation. Figure 7 presents a comparatively larger variation in c_{in} and σ for galaxy pairs that have smaller relative velocity, suggesting an inverse correlation between tidal energy deposits in a galaxy and velocity difference between pairs (Barton et al. 2000; Park & Choi 2009). The overall small variation in structural properties as a function of environments as evident in Figure 8 suggests these are less closely related to their "environments" than are their masses and star formation histories (see e.g. Blanton et al. 2005b; van der Wel 2008).

Major outcomes of our studies are as follows.

- The properties of passive galaxies that are separated more than the one virial radius of the nearest neighbor are independent of the separation. Initial dependence of physical property on the separation starts as soon as the galaxy enters the neighbor's virial radius with another change occurring at about $0.1 r_{vir,nei}$, which corresponds to $20 - 30 h^{-1} \text{kpc}$ for galaxies in our sample.
- We do not observe a morphology density relation (Dressler 1980) for passive galaxies in low density environments as indicated by nearly horizontal, constant f_E contours in Figure 2. The galaxy morphology mainly depends on the pair separation combined with morphology of the neighbor galaxy.
- Only luminosity of the passive galaxies show a dependence on ρ_{20} (Figure 4) especially at separations larger than virial radius of the neighbor. This corroborates the evidence regarding transforma-

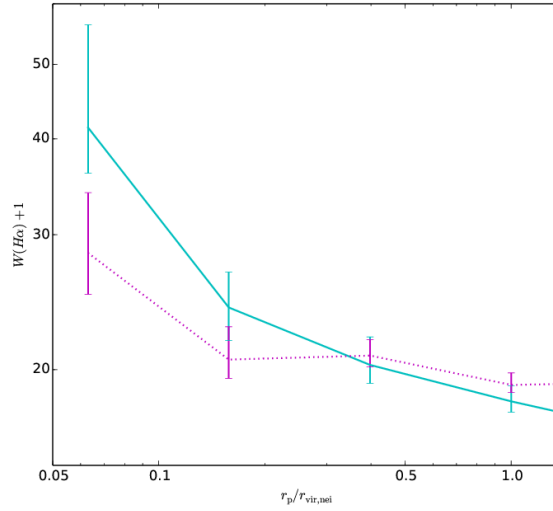


Figure 9. Dependence of $W(H\alpha) - r_p/r_{vir,nei}$ relation on the absolute magnitude of the neighbor galaxy for late type galaxies with late type neighbors. The solid cyan line is for the target galaxies having neighbors that are up to one magnitude fainter ($\Delta M_r = 1$), and dotted magenta line is for galaxies having neighbors that are up to one magnitude brighter ($\Delta M_r = -1$) than the target itself. The r_p -space is uniformly binned in the logarithmic scale and in each bin, late type galaxies with axis ratio of $b/a \geq 0.6$ are selected for the median $W(H\alpha)$ curve.

tion of luminosities of passive galaxies through mergers (Park & Choi 2009).

- At fixed morphology and luminosity, both SF activity as well as structural parameter of galaxies show a weak or negligible dependence on ρ_{20} . Variations in neighbor absolute magnitude does not vary the star formation activity of the target galaxy considerably (Figure 9). The weak residual dependence on ρ_{20} of the $u - r$ color of galaxies can be attributed to the presence of hotter and denser halo gas in galaxies in high density environments.

ACKNOWLEDGMENTS

JKY thanks Changbom Park and Yun-Young Choi for many useful discussions and suggestions. JKY acknowledges financial support from Chinese Academy of Sciences for fellowship assistance during this work. JKY and XC acknowledge support from NSFC via project number 11250110510 and 11373030 respectively. Funding for the SDSS and SDSS-II was provided by the Alfred P. Sloan Foundation, the Participating Institutions, the National Science Foundation, the U.S. Department of Energy, the National Aeronautics and Space Administration, the Japanese Monbukagakusho, the Max Planck Society, and the Higher Education Funding Council for England. The SDSS was managed by the Astrophysical Research Consortium for the Participating Institutions.

REFERENCES

- Abazajian, K. N., Adelman-McCarthy, J. K., Agüeros, M. A., et al. 2009, *ApJS*, 182, 543
- Abell, G. O., Corwin, H. G., Jr., & Olowin, R. P. 1989, *ApJS*, 70, 1
- Ann, H. B., Park, C., & Choi, Y.-Y. 2008, *MNRAS*, 389, 86
- Bahcall, N. A., Soneira, R. M., & Burgett, W. S. 1986, *ApJ*, 311, 15
- Ball, N. M., Loveday, J., & Brunner, R. J. 2008, *MNRAS*, 383, 907
- Balogh, M., Eke, V., Miller, C., et al. 2004, *MNRAS*, 348, 1355
- Bamford, S. P., Rojas, A. L., Nichol, R. C., et al. 2008, *MNRAS*, 391, 607
- Barton, E. J., Geller, M. J., & Kenyon, S. J. 2000, *ApJ*, 530, 660
- Barton, E. J., Arnold, J. A., Zentner, A. R., Bullock, J. S., & Wechsler, R. H. 2007, *ApJ*, 671, 1538
- Binggeli, B. 1982, *A&A*, 107, 338
- Binney, J., & Tremaine, S. 1987, Princeton, NJ, Princeton University Press, 1987, 747 p.,
- Blanton, M. R., Lin, H., Lupton, R. H., et al. 2003, *AJ*, 125, 2276
- Blanton, M. R., Schlegel, D. J., Strauss, M. A., et al. 2005, *AJ*, 129, 2562
- Blanton, M. R., Lupton, R. H., Schlegel, D. J., et al. 2005b, *ApJ*, 631, 208
- Blanton, M. R., & Berlind, A. A. 2007, *ApJ*, 664, 791
- Blanton, M. R., & Moustakas, J. 2009, *ARA&A*, 47, 159
- Bretherton, C. F., Moss, C., & James, P. A. 2013, *A&A*, 553, A67
- Buta, R. J. 2013, *Planets, Stars and Stellar Systems. Volume 6: Extragalactic Astronomy and Cosmology*, 1
- Carter, B. J., Fabricant, D. G., Geller, M. J., Kurtz, M. J., & McLean, B. 2001, *ApJ*, 559, 606
- Cervantes-Sodi, B., Park, C., Hernandez, X., & Hwang, H. S. 2011, *MNRAS*, 414, 587
- Choi, Y.-Y., Park, C., & Vogeley, M. S. 2007, *ApJ*, 658, 884
- Choi, Y.-Y., Han, D.-H., & Kim, S. S. 2010, *Journal of Korean Astronomical Society*, 43, 191
- Christlein, D., & Zabludoff, A. I. 2005, *ApJ*, 621, 201
- Condon, J. J., Condon, M. A., Gisler, G., & Puschell, J. J. 1982, *ApJ*, 252, 102
- Cooper, M. C., Newman, J. A., Croton, D. J., et al. 2006, *MNRAS*, 370, 198
- Cooper, M. C., Griffith, R. L., Newman, J. A., et al. 2012, *MNRAS*, 419, 3018
- Croton, D. J., & Farrar, G. R. 2008, *MNRAS*, 386, 2285

- Cucciati, O., Iovino, A., Marinoni, C., et al. 2006, *A&A*, 458, 39
- Dressler, A. 1980, *ApJ*, 236, 351
- Einasto, M., Einasto, J., Tago, E., et al. 2007, *A&A*, 464, 815
- Ellison, S. L., Nair, P., Patton, D. R., et al. 2011, *MNRAS*, 416, 2182
- Faber, S. M., & Jackson, R. E. 1976, *ApJ*, 204, 668
- Fukugita, M., Ichikawa, T., Gunn, J. E., et al. 1996, *AJ*, 111, 1748
- Gómez, P. L., Nichol, R. C., Miller, C. J., et al. 2003, *ApJ*, 584, 210
- Gunn, J. E., Carr, M., Rockosi, C., et al. 1998, *AJ*, 116, 3040
- Harrison, C. D., Colless, M., Kuntschner, H., et al. 2011, *MNRAS*, 413, 1036
- Hernández-Toledo, H. M., Avila-Reese, V., Conselice, C. J., & Puerari, I. 2005, *AJ*, 129, 682
- Hirschmann, M., De Lucia, G., Iovino, A., & Cucciati, O. 2013, *MNRAS*, 433, 1479
- Hubble, E. P. 1936, *Realm of the Nebulae*, by E.P. Hubble. New Haven: Yale University Press, 1936. ISBN 9780300025002,
- Huertas-Company, M., Mei, S., Shankar, F., et al. 2013, *MNRAS*, 428, 1715
- Ideue, Y., Taniguchi, Y., Nagao, T., et al. 2012, *ApJ*, 747, 42
- Kajisawa, M., Shioya, Y., Aida, Y., et al. 2013, *ApJ*, 768, 51
- Kauffmann, G., White, S. D. M., Heckman, T. M., et al. 2004, *MNRAS*, 353, 713
- Keel, W. C., Kennicutt, R. C., Jr., Hummel, E., & van der Hulst, J. M. 1985, *AJ*, 90, 708
- Kennicutt, R. C., Jr., Roettiger, K. A., Keel, W. C., van der Hulst, J. M., & Hummel, E. 1987, *AJ*, 93, 1011
- Kennicutt, R. C., Jr. 1998, *ApJ*, 498, 541
- Lambas, D. G., Alonso, S., Mesa, V., & O'Mill, A. L. 2012, *A&A*, 539, A45
- Lani, C., Almaini, O., Hartley, W. G., et al. 2013, *MNRAS*, 435, 207
- Larson, R. B., & Tinsley, B. M. 1978, *ApJ*, 219, 46
- Lewis, I., Balogh, M., De Propriis, R., et al. 2002, *MNRAS*, 334, 673
- Lietzen, H., Tempel, E., Heinämäki, P., et al. 2012, *A&A*, 545, A104
- Lupton, R. H., Gunn, J. E., & Szalay, A. S. 1999, *AJ*, 118, 1406
- Lupton, R., Gunn, J. E., Ivezić, Z., Knapp, G. R., & Kent, S. 2001, *Astronomical Data Analysis Software and Systems X*, 238, 269
- Mahajan, S., Haines, C. P., & Raychaudhury, S. 2010, *MNRAS*, 404, 1745
- Mateus, A., & Sodré, L. 2004, *MNRAS*, 349, 1251
- McQuinn, K. B. W., Skillman, E. D., Cannon, J. M., et al. 2010, *ApJ*, 721, 297
- Monaghan, J. J., & Lattanzio, J. C. 1985, *A&A*, 149, 135
- Muldrew, S. I., Croton, D. J., Skibba, R. A., et al. 2012, *MNRAS*, 419, 2670
- Nikolic, B., Cullen, H., & Alexander, P. 2004, *MNRAS*, 355, 874
- Oemler, A., Jr. 1974, *ApJ*, 194, 1
- Park, C., & Choi, Y.-Y. 2005, *ApJL*, 635, L29
- Park, C., Choi, Y.-Y., Vogeley, M. S., et al. 2007, *ApJ*, 658, 898
- Park, C., Gott, J. R., III, & Choi, Y.-Y. 2008, *ApJ*, 674, 784
- Park, C., & Choi, Y.-Y. 2009, *ApJ*, 691, 1828
- Park, C., & Hwang, H. S. 2009, *ApJ*, 699, 1595
- Patel, S. G., Kelson, D. D., Holden, B. P., Franx, M., & Illingworth, G. D. 2011, *ApJ*, 735, 53
- Patton, D. R., Grant, J. K., Simard, L., et al. 2005, *AJ*, 130, 2043
- Patton, D. R., Ellison, S. L., Simard, L., McConnachie, A. W., & Mendel, J. T. 2011, *MNRAS*, 412, 591
- Postman, M., & Geller, M. J. 1984, *ApJ*, 281, 95
- Shimasaku, K., Fukugita, M., Doi, M., et al. 2001, *AJ*, 122, 1238
- Skibba, R. A., Masters, K. L., Nichol, R. C., et al. 2012, *MNRAS*, 423, 1485
- Spitzer, L., Jr., & Baade, W. 1951, *ApJ*, 113, 413
- Strateva, I., Ivezić, Ž., Knapp, G. R., et al. 2001, *AJ*, 122, 1861
- Strauss, M. A., Weinberg, D. H., Lupton, R. H., et al. 2002, *AJ*, 124, 1810
- Struck, C. 2006, *Astrophysics Update* 2, 115
- Tully, R. B., & Fisher, J. R. 1977, *A&A*, 54, 661
- Tonnesen, S., & Cen, R. 2012, *MNRAS*, 425, 2313
- Toomre, A. 1977, *Evolution of Galaxies and Stellar Populations*, 401
- van der Wel, A. 2008, *ApJL*, 675, L13
- Wang, Y., Park, C., Hwang, H. S., & Chen, X. 2010, *ApJ*, 718, 762
- Weinmann, S. M., van den Bosch, F. C., Yang, X., & Mo, H. J. 2006, *MNRAS*, 366, 2
- White, M., Cohn, J. D., & Smit, R. 2010, *MNRAS*, 408, 1818
- Woods, D. F., & Geller, M. J. 2007, *AJ*, 134, 527
- Yang, X., Mo, H. J., van den Bosch, F. C., et al. 2007, *ApJ*, 671, 153